

Impact of CO₂/N₂/Ar Addition on the Internal Structure and Stability of Non-Premixed CH₄/Air flames at liftoff

Jiesheng Min¹, Aurélie Wyzgolik¹, Françoise Baillot¹, Eric Domingues¹
Martine Talbaut¹, Béatrice Patte-Rouland¹

¹ Laboratory CORIA – UMR 6614, CNRS-Université et INSA de Rouen, France

AND

Dany Escudié², Cédric Galizzi², Frédéric André², Olivier Gicquel³

²Laboratory CETHIL - UMR 5008, CNRS-INSA de Lyon, France

³Laboratory EM2C - UPR 288 CNRS, Ecole Centrale Paris, France

1 Introduction

Exhaust gas recirculation combustion systems are widely used nowadays for their great combustion efficiency and the very reduced NO_x emission. It is known that among the exhaust combustion gases, CO₂ and H₂O are of paramount importance, because of their physico-chemical properties and their great amount. The present study is focused on the influence of carbon dioxide added to the air on the transition from an attached flame to a lifted flame. As it is shown in the literature [1, 2, 3] the main effects due to the presence of a diluent are induced not only by pure dilution, but also by thermal and chemical actions. In order to find features able to discriminate between them, two other diluents have also been investigated: nitrogen, thermally inert and argon, chemically inert.

2 Experimental Configuration

Here, experiments are carried out in the CORIA laboratory. Flames develop in a long atmospheric vertical square test chamber. Five windows, aligned vertically, have been dug in each of two opposite sides of the chamber to place glass monitors for visualization or plates instrumented with thermocouples. Two slits, centered at the base of its two other walls, allow a laser sheet to pass through the chamber. Its 0.25m² section through which the oxide is injected, is large enough to prevent the interaction between the flame and the walls. A round tube with an inner diameter, $D_i = 6\text{mm}$, a 1m length and a thick lip, $e_1 = 2.1\text{mm}$ is centered inside the furnace such that methane is injected at the bottom of the test chamber. The oxide used here is either pure air or air diluted with CO₂, N₂ or Ar. Gases are well mixed in a blender before entering the furnace by four inlets located at the base of a quiet chamber (more details in [4]). Oxide and methane flow rate velocities are $0.1\text{m/s} < U_{\text{oxide}} < 0.67\text{m/s}$ and $1\text{m/s} < U_{\text{CH}_4} < 20\text{m/s}$ respectively. Three optical techniques were used to investigate flame properties: shadowgraph method, CH* chemiluminescence imaging, planar OH Laser Induced Fluorescence. Shadowgraph method visualizes the interfaces between hot and fresh gases which are recorded by a Phantom camera ($\leq 2000\text{fps}$, 1600×1200 pixels). Direct CH* emission of the flame,

collected by an ICCD Princeton camera (1fps, 576×384 pixels, 16bits, exposure time: 250μs, 0.08mm/pixel) equipped with an interferential filter centered at 430nm with FWHM 50nm, is used to measure the flame attachment height. The OH-PLIF signal is collected by an ICCD Princeton PI-Max camera (10fps, 16bits, 512*512 pixels, exposure time: 50ns, 0.08 mm/pixel). It is equipped with a 105mm UV lens and two glass filters (WG305 & UG11) to eliminate scattering and flame radiations. The raw OH-PLIF images are corrected for the background and spatial laser beam intensity variations.

3 Charts of Flame Stability

First, lifting process during which the flame detaches from the burner is investigated for a non-diluted configuration by increasing U_{CH_4} gradually for a fixed U_{air} . Methane velocities needed for the flame reattachment, U_a are lower than those for lifting, U_l [5]. This hysteresis phenomenon describes a zone in which the flame is either attached at or lifted above the burner (see Fig. 1). This zone is considered as a reference for the flame stability study when a diluent is added.

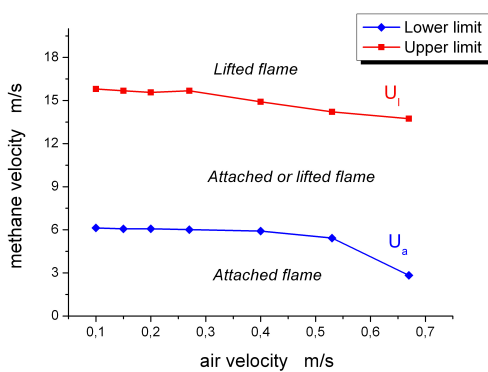


Figure 1. Hysteresis zone without dilution

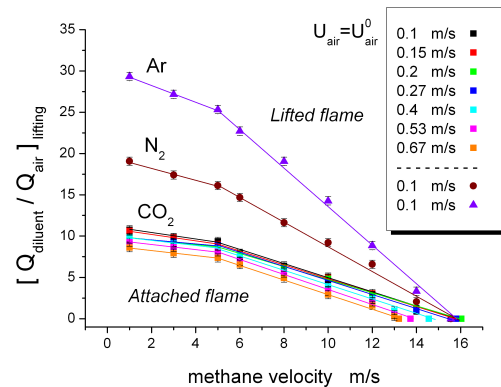


Figure 2. Lifting limits with CO₂, N₂ or Ar dilution

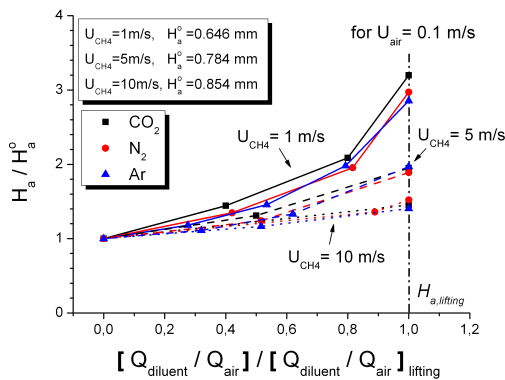


Figure 3. H_a/H_a^0 vs. normalized flow rate ratio

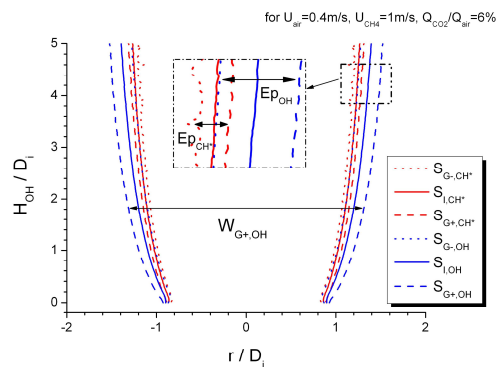


Figure 4. Inner flame structure: CH*, OH lines

Contrary to the pure air case, lifting systematically occurs, provided that a critical quantity of diluent added to the air, expressed through the flow rate ratio $(Q_{diluent}/Q_{air})_{lifting}$, is attained. To delimit the mechanical impact due to species addition, three experimental procedures were proposed: 1) constant oxygen mass, 2) constant oxide flow rate velocity (shear strain at the oxide/fuel interface) and 3) constant oxide mass. As reported in [4], results with the three procedures differ no more than 5% despite velocity and mass augmentations about 10% with CO₂ (20% with N₂ and 30% with Ar) between procedures (1) and (2), and about 15% with CO₂ (19% with N₂ and 41% with Ar) between procedures (1) and (3). So, mechanical impact is minor in the lifting process by a diluent. Fig.2 shows critical flow rate ratio $(Q_{diluent}/Q_{air})_{lifting}$ data obtained at lifting with procedure (1) as functions of U_{CH_4} . $(Q_{diluent}/Q_{air})_{lifting}$ strongly depends on U_{CH_4} , but less on U_{air} due to the narrow range of values imposed to U_{air} . All the profiles have the same trend: a slow decrease with $U_{CH_4} \leq 5$ m/s,

followed by a steeper one until the natural lifting velocity is reached. This transitional behavior in flame lifting relates to the change of methane jet regime from laminar to turbulent. So, inner aerodynamic instabilities promote flame stability loss. Equally, experiments with N_2 or Ar lead to lift off the flame in the same range (U_{CH_4} , U_{air}), but the critical ratios $(Q_{N_2}/Q_{air})_{lifting}$ and $(Q_{Ar}/Q_{air})_{lifting}$ are two and three times greater than $(Q_{CO_2}/Q_{air})_{lifting}$, indicating a better stability with these diluents. The critical ratios' ranking confirms those obtained by Takahashi et al. [2] in a fire extinguishment study with very slow velocities ($U_{air}=0.0092$ m/s, 0.05 m/s $< U_{CH_4} < 0.2$ m/s): it follows the order of the diluent molar heat capacities. To quantify stability loss, several typical flame quantities are studied as a diluent is added.

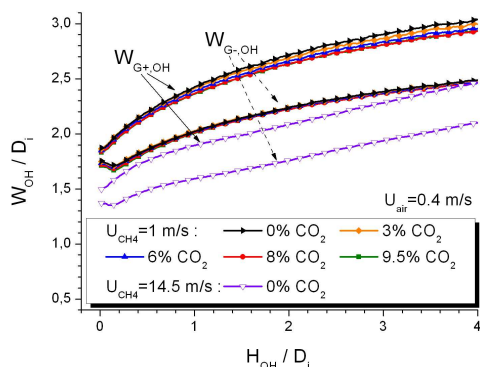
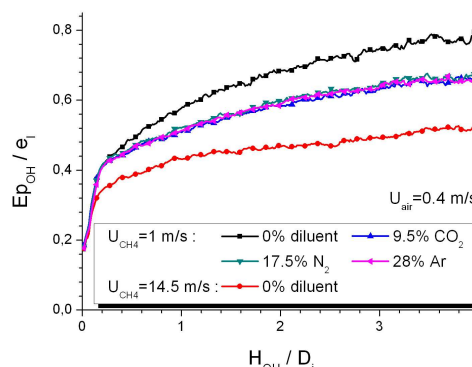
4 Flame attachment height

The attachment height, H_a (H_a^0 with no dilution) defined as the distance between the flame base and the burner exit is obtained from direct CH^* emission images [4]. The measurement uncertainty is ± 1 pixel. When a diluent is added to the air, the flame, still anchored, is pushed away and stabilizes at a downstream position. Results in Fig. 3 show that $Q_{diluent}/Q_{air}$ essentially controls H_a for a given (U_{CH_4} , U_{air}): whatever the diluent, H_a/H_a^0 evolves as a unique function of $Q_{diluent}/Q_{air}$ normalized by $(Q_{diluent}/Q_{air})_{lifting}$. For the greatest flow rate ratios, H_a always exceeds the maximal no-diluted attachment height, $H_{a,lifting}^0$, obtained at lifting. Finally, lifting occurs at a unique critical height $H_{a,lifting}/H_a^0$. In order to check this increase is not caused by "classical" aerodynamic effects, the three procedures were applied for all the conditions. All the series of profiles were found to have the same trend as that in Fig. 3. Discrepancies due to the procedures are less than 5% on average, which is of the same order of magnitude as the measurement uncertainty mentioned above. On the other hand, when U_{air} or U_{CH_4} is increased, as clearly shown in Fig. 3, aerodynamics opposes dilution effect on H_a by inducing its diminishing. Thus, $(Q_{diluent}/Q_{air})/(Q_{diluent}/Q_{air})_{lifting}$ appears as a key element in a scenario involving a dilution mechanism in the flame stabilization process.

5 Inner flame Structure: OH, CH^*

How the inner flame structure responds to the presence of a diluent is quantified through the spatial evolution of OH and CH^* species. To do that, OH-LIF and direct CH^* emission images are simultaneously captured near its base. Analysis and image processing are those proposed by Wyzgolik & Baillot, and will not be discussed here. Lines of specific OH and CH^* surfaces are identified: lines of the maximum OH-LIF intensity surfaces, $S_{I,OH}$, of the maximum OH-LIF intensity gradient surfaces on the air side, $S_{G+,OH}$ and on the methane side, $S_{G-,OH}$; the same description is made for CH^* emission: S_{I,CH^*} , S_{G+,CH^*} , S_{G-,CH^*} . All these surfaces are correctly described by their widths (or diameters): $W_{I,OH}$, W_{I,CH^*} , $W_{G+,OH}$, $W_{G-,OH}$, W_{G+,CH^*} and W_{G-,CH^*} . The thickness of the OH radical zone, Ep_{OH} is delimited by $S_{G+,OH}$ and $S_{G-,OH}$, and the thickness of the CH^* radical zone Ep_{CH^*} is delimited by S_{G+,CH^*} and S_{G-,CH^*} . All the parameters, extracted from images, are defined in Fig. 4 with r the radial distance from the burner axis. H_{OH} , the vertical distance from the base of an OH-surface, is also introduced. As determined experimentally by Wyzgolik & Baillot in a non-diluted configuration, the OH-zone of thickness, Ep_{OH} partly overlaps the CH^* -zone of thickness Ep_{CH^*} such that $S_{G-,OH}$ coincides with S_{I,CH^*} (see Fig.4). Fig. 5 illustrates the typical evolution of $W_{G+,OH}$, $W_{G-,OH}$ for $U_{air} = 0.4$ m/s without and with CO_2 dilution. First, the pure aerodynamics influence is quantified by comparing widths measured with no-dilution at a low fuel velocity ($U_{CH_4} = 1$ m/s) and at lifting ($U_{CH_4} = 14.5$ m/s): increasing shear strain on fuel side leads to the global narrowing of surfaces $S_{G+,OH}$ and $S_{G-,OH}$ toward the fuel ($W_{G+,OH}$ and $W_{G-,OH}$ diminish by $\sim e_1$ at every locations H_{OH}), while H_a^0 increases only from 0.77 to 0.93 mm (16% width diminishing). At the same time, thickness Ep_{OH} drastically diminishes by $\sim 30\%$ even at the flame base, $H_{OH} \sim 0$ (see Fig.6). Secondly, diluted combustion is analyzed by comparing non-diluted widths with those obtained with CO_2 diluent (N_2 and Ar are not presented here). The flame response is totally different: whatever the diluent, $S_{G+,OH}$ narrows toward methane when $Q_{diluent}/Q_{air}$ is increased, while $S_{G-,OH}$ deviates just a little. So, the side on which a diluent is added is crucial: there is a

preferential diffusion of the diluent, which is consistent with [1, 3]. But, as shown in Fig.5, the global narrowing of $S_{G+,OH}$ does no more exist: diluent progressively affects $W_{G+,OH}$ as H_{OH} is increased. With a diluent, the growth of Ep_{OH} vs. H_{OH} , reported in Fig. 6, is slowed down gradually from $H_{OH} \sim 0$ at which the value is unchanged compared to that one measured with no-dilution under the same velocity condition. Whatever the diluent, Ep_{OH} evolves identically at lifting: $(Q_{diluent}/Q_{air})_{lifting}$ controls Ep_{OH} as it does for H_a . Thus, flame structure is differently modified during the two lifting processes. All these features are noted in the entire (U_{CH_4}, U_{air}) range.

Figure 5. W_{OH} vs. H_{OH} Figure 6. Ep_{OH} vs. H_{OH}

6 Conclusion

Flame lifting is shown to be controlled essentially by the critical flow rate ratio, $Q_{diluent}/Q_{air}$, even though aerodynamics from inner jet structure does influence it. Numerical results based on Guo's simulation presented at Icders 2009, successfully fitting with our laminar results, highlight the relative contribution of the three phenomena (dilution, thermal and chemistry) induced by a diluent. With dilution flames can exist at a higher position, H_a . Its evolution is dictated by $(Q_{diluent}/Q_{air})/(Q_{diluent}/Q_{air})_{lifting}$ for the three diluents. In agreement with Takahashi et al., adding diluent reduces the reaction rate near the edge flame; the balance between the combustion propagation speed and flow injection velocity is broken. Then, a new balance is found downstream which stabilizes the flame. In such a scenario, for given aerodynamic conditions, $H_{a,lifting}$ measured here is the maximum sustainable height at $(Q_{diluent}/Q_{air})_{lifting}$. Modifications of inner flame structures are different when lifting results from pure aerodynamics or diluent addition. Lifting scenarios are distinct, based on specific mechanisms.

References

- [1] Lock A., Briones A.M., Aggarwal S.K., Puri I.K., Hegde U. (2007). Liftoff and extinction characteristics of fuel- and air-stream-diluted methane-air flames. *Combustion and Flame* 149: 340
- [2] Takahashi, F., Linteris, G.T., Katta, V.R. (2007). Extinguishment mechanisms of coflow diffusion flames in a cup-burner apparatus. *Proc. Comb. Inst.* 31: 2721
- [3] Liu F., Guo H., Samalwood G.J., Gulder O. (2001). The chemical effects of carbon dioxide as an additive in an ethylene diffusion flame. *Combustion and Flame* 125: 778
- [4] Min J., Baillot F., Domingues E., Patte-Rouland B., Talbaut M., Escudié D., Galizzi C., André F., Gicquel O. (2008). Effect of CO_2 addition on the stability and the flickering of non-premixed methane/air flames. The 19th Int. Symposium on Transport Phenomena. Reykjavik, ICELAND
- [5] Wyzgolik A., Baillot F. (2007). Response of the non-premixed lifted flame to coaxial jet mixing layers. *Proc. Comb. Inst.* 31:1583